

A Variational Asymptotic Micromechanics Model for Predicting Thermoelastic Properties of Heterogeneous Materials

Wenbin Yu¹ and Tian Tang

*Department of Mechanical and Aerospace Engineering
Utah State University, Logan, Utah 80322-4130, USA*

Abstract

A variational asymptotic micromechanics model has been developed for predicting effective thermoelastic properties of composite materials, and recover the local fields within the unit cell. This theory adopts essential assumptions within the concept of micromechanics, achieves an excellent accuracy, and provides a unified treatment for one-dimensional, two-dimensional, and three-dimensional unit cells. This theory is implemented using the finite element method into the computer program, VAMUCH, a general-purpose micromechanics analysis code. Several examples are used to validate the theory and the code. The results are compared with those available in the literature and those produced by a commercial finite element package.

Key words: Heterogeneous; Thermoelastic; Micromechanics; Homogenization; Variational Asymptotic Method

1 Introduction

In recent years, more and more structures are made of composite materials with engineered microstructure for better performance. Because the macroscopic structural dimensions are usually several orders of magnitude larger than the characteristic size of constituents, it is not very practical to analyze such structures by meshing all the details of constituent materials. Usually, the concept of unit cell (UC) is used to create a pseudo, “effective”, material with homogeneous properties from the original heterogeneous materials with so-called micromechanics models; see Figure 1.

¹ Corresponding author: +1-435-7978246 (tel.); +1-435-7972417 (fax)
Email address: wenbin.yu@usu.edu (Wenbin Yu).

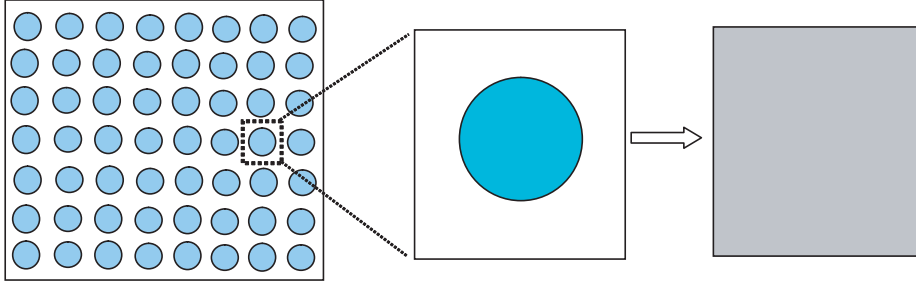


Fig. 1. Heterogenous material, unit cell, and effective material

In the past several decades, numerous micromechanics models have been developed; see Hashin (1983) and references cited therein. The simplest models are the rules of mixture based on Voigt and Reuss hypotheses, which provides the upper and lower bounds, respectively (Hill, 1952). The difference between these two bounds could be too large to be useful for general composite materials. To this end, researchers have proposed various techniques to either reduce the difference between the bounds, or find an approximate value between the upper and lower bounds. Typical approaches are the self-consistent model (Hill, 1965) and its generalizations (Dvorak and Bahei-El-Din, 1979; Accorsi and Nemat-Nasser, 1986), the variational approach of Hashin and Shtrikman (Hashin and Shtrikman, 1962), third-order bounds (Milton, 1981), the method of cells (MOC) (Aboudi, 1982) and its variants (Aboudi, 1989; Paley and Aboudi, 1992; Aboudi et al., 2001; Williams, 2005b), recursive cell method (Banerjee and Adams, 2004), mathematical homogenization theories (MHT) (Bensoussan et al., 1978; Murakami and Toledano, 1990), finite element approaches using conventional stress analysis of a representative volume element (RVE) (Sun and Vaidya, 1996), and many others. Although these approaches were originally introduced to predict elastic properties, most of these approaches are also extended to predict thermomechanical properties; see Schapery (1968), Rosen and Hashin (1970), and Aboudi (1984) for a few examples.

Recently, a new technique for micromechanics modeling, namely variational asymptotic method for unit cell homogenization (VAMUCH) (Yu and Tang, 2007), has been developed based on the variational asymptotic method of Berdichevsky (1979). The technique invokes two essential assumptions within the concept of micromechanics:

- **Assumption 1** The exact solutions of the field variables have volume averages over the UC. For example, if u_i are the exact displacements within the UC, there exist v_i such that

$$v_i = \frac{1}{\Omega} \int_{\Omega} u_i \, d\Omega \equiv \langle u_i \rangle \quad (1)$$

where Ω denotes the domain occupied by the UC and its volume.

- **Assumption 2** The effective material properties obtained from the micromechanical analysis of the UC are independent of the geometry, the boundary conditions, and loading conditions of the macroscopic structure, which means that effective material properties are assumed to be the intrinsic properties of the material when viewed macroscopically.

Please note these assumptions are not restrictive. The mathematical meaning of the first assumption is that the exact solutions of the field variables are integrable over the domain of UC, which is true almost all the time. The second assumption implies that we can neglect the size effects of the material properties in the macroscopic analysis, which is an assumption often made in the conventional continuum mechanics. Of course, the micromechanical analysis of the UC is only needed and appropriate if $\eta = h/l \ll 1$, with h as the characteristic size of the UC and l as the characteristic wavelength of the deformation of the macroscopic material.

In this paper, we will first use this modeling technique to construct a new micromechanics model for effective thermoelastic properties including elastic properties, coefficients of thermal expansion (CTEs), and specific heat for heterogeneous materials. Then we will implement the theory using the finite element method in the computer program VAMUCH to provide engineers with a general-purpose micromechanics tool for thermoelastic micromechanical analysis of composite materials.

2 Theoretical Formulation

We need to use three coordinate systems: two cartesian coordinates $\mathbf{x} = (x_1, x_2, x_3)$ and $\mathbf{y} = (y_1, y_2, y_3)$, and an integer-valued coordinate $\mathbf{n} = (n_1, n_2, n_3)$; see Figure 2. We use x_i as the global coordinates to describe the macroscopic material and y_i parallel to x_i as the local coordinates to describe the UC. Here and throughout the paper, Latin indices assume 1, 2, and 3 and repeated indices are summed over their range except where explicitly indicated. We choose the origin of the local coordinates y_i to be the geometric center of UC. For example, if the UC is a cube with dimensions as d_i , then $y_i \in [-\frac{d_i}{2}, \frac{d_i}{2}]$. To uniquely locate a UC in the composite material, we also introduce integer coordinates n_i . The integer coordinates are related to the global coordinates in such a way that $n_i = x_i/d_i$ (no summation over i).

As implied by Assumption 2, we can obtain the same effective properties from an imaginary, unbounded, and unloaded composite material with the same microstructure as the real, loaded, and bounded one. Hence we could derive the micromechanics model from an imaginary, unloaded, composite material which completely occupies the three-dimensional (3D) space \mathcal{R} and composes

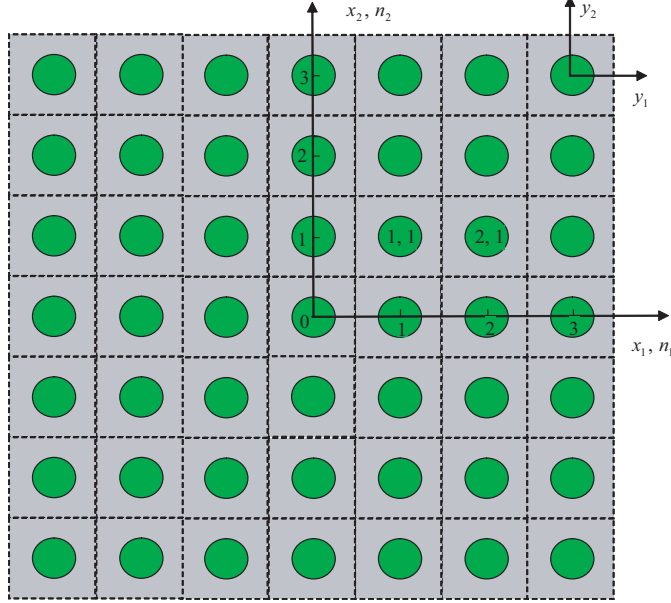


Fig. 2. Coordinate systems for heterogenous materials (only two-dimensional (2D) UC is drawn for clarity)

of infinite many repeating UCs. The total generalized potential energy of this imaginary material is equal to the summation of the Helmholtz free energy (Rosen and Hashin, 1970) stored in all the UCs, which is:

$$\Pi = \sum_{n=-\infty}^{\infty} \frac{1}{2} \int_{\Omega} (C_{ijkl} \epsilon_{ij} \epsilon_{kl} + 2\beta_{ij} \epsilon_{ij} \theta + c_v \frac{\theta^2}{T_0}) d\Omega \quad (2)$$

where C_{ijkl} are components of the fourth-order elasticity tensor, β_{ij} are second-order tensor of thermal stress coefficients, c_v is the specific heat per unit volume at constant volume, T_0 is the reference temperature at which the constituent material is stress free, θ denotes the difference between the actual temperature and the reference temperature, and ϵ_{ij} are the components of the 3D strain tensor defined for the linear theory as

$$\epsilon_{ij}(\mathbf{n}; \mathbf{y}) = \frac{1}{2} \left[\frac{\partial u_i(\mathbf{n}; \mathbf{y})}{\partial y_j} + \frac{\partial u_j(\mathbf{n}; \mathbf{y})}{\partial y_i} \right] \quad (3)$$

In view of the fact that these infinite many UCs form a continuous heterogeneous material, we need to enforce the continuity of the displacement field u_i on the interface between adjacent UCs, which can be written as follows for a UC with integer coordinates (n_1, n_2, n_3) :

$$\begin{aligned} u_i(n_1, n_2, n_3; d_1/2, y_2, y_3) &= u_i(n_1 + 1, n_2, n_3; -d_1/2, y_2, y_3) \\ u_i(n_1, n_2, n_3; y_1, d_2/2, y_3) &= u_i(n_1, n_2 + 1, n_3; y_1, -d_2/2, y_3) \\ u_i(n_1, n_2, n_3; y_1, y_2, d_3/2) &= u_i(n_1, n_2, n_3 + 1; y_1, y_2, -d_3/2) \end{aligned} \quad (4)$$

For the purpose to obtain the effective CTEs and specific heat of composite

materials, we assume that θ is constant with respect to time and space coordinates, which is a common practice in the literature; see Rosen and Hashin (1970) for example. Hence the continuity condition for temperature field between adjacent UCs is automatically satisfied. According to the principle of minimum total potential energy, the exact solution will minimize the energy in Eq. (2) under the constraints in Eq. (1) and Eqs. (4). To avoid the difficulty associated with discrete integer arguments, we can reformulate the problem, including Eqs. (2), (3), and (4), in terms of continuous functions using the idea of quasicontinuum introduced in Kunin (1982) as:

$$\Pi = \frac{1}{2} \int_{\mathcal{R}} \left\langle C_{ijkl} \epsilon_{ij} \epsilon_{kl} + 2\beta_{ij} \epsilon_{ij} \theta + c_v \frac{\theta^2}{T_0} \right\rangle d\mathcal{R} \quad (5)$$

$$\epsilon_{ij}(\mathbf{x}; \mathbf{y}) = \frac{1}{2} \left[\frac{\partial u_i(\mathbf{x}; \mathbf{y})}{\partial y_j} + \frac{\partial u_j(\mathbf{x}; \mathbf{y})}{\partial y_i} \right] \equiv u_{(i|j)} \quad (6)$$

and

$$\begin{aligned} u_i(x_1, x_2, x_3; d_1/2, y_2, y_3) &= u_i(x_1 + d_1, x_2, x_3; -d_1/2, y_2, y_3) \\ u_i(x_1, x_2, x_3; y_1, d_2/2, y_3) &= u_i(x_1, x_2 + d_2, x_3; y_1, -d_2/2, y_3) \\ u_i(x_1, x_2, x_3; y_1, y_2, d_3/2) &= u_i(x_1, x_2, x_3 + d_3; y_1, y_2, -d_3/2) \end{aligned} \quad (7)$$

Using the technique of Lagrange multipliers, we can pose the thermoelastic analysis as a stationary value problem of the following functional:

$$\begin{aligned} J = \int_{\mathcal{R}} \left\{ \left\langle \frac{1}{2} C_{ijkl} u_{(i|j)} u_{(k|l)} + \beta_{ij} u_{(i|j)} \theta + \frac{1}{2} c_v \frac{\theta^2}{T_0} \right\rangle \right. \\ \left. + \lambda_i (\langle u_i \rangle - v_i) + \int_{S_1} \gamma_{i1} (u_i^{+1} - u_i^{-1}) dS_1 \right. \\ \left. + \int_{S_2} \gamma_{i2} (u_i^{+2} - u_i^{-2}) dS_2 + \int_{S_3} \gamma_{i3} (u_i^{+3} - u_i^{-3}) dS_3 \right\} d\mathcal{R} \end{aligned} \quad (8)$$

with

$$u_i^{+j} = u_i|_{y_j=d_j/2}, \quad u_i^{-j} = u_i|_{x_j=x_j+d_j, y_j=-d_j/2} \quad \text{for } j = 1, 2, 3$$

where λ_i and γ_{ij} are Lagrange multipliers introducing constraints in Eqs. (1) and (7), respectively, and S_i are the surfaces with $n_i = 1$. The main objective of micromechanics is to find the real displacements u_i in terms of v_i , which is a very difficult problem because we have to solve this stationary problem for each point in the global system x_i as in Eq. (8). It will be desirable if we can formulate the variational statement posed over a single UC only. In view of Eq. (1), it is natural to express the exact solution u_i as a sum of the volume average v_i plus the difference, such that

$$u_i(\mathbf{x}; \mathbf{y}) = v_i(\mathbf{x}) + w_i(\mathbf{x}; \mathbf{y}) \quad (9)$$

where $\langle w_i \rangle = 0$ according to Eq. (1). The very reason that the heterogenous material can be homogenized leads us to believe that w_i should be asymptotically smaller than v_i , *i.e.*, $w_i \sim \eta v_i$. Substituting Eq. (9) into Eq. (8) and making use of Eqs (6), we can obtain the leading terms of the functional as:

$$\begin{aligned}
J_1 = \int_{\mathcal{R}} \left\{ \left\langle \frac{1}{2} C_{ijkl} w_{(i|j)} w_{(k|l)} + \beta_{ij} w_{(i|j)} \theta + \frac{1}{2} c_v \frac{\theta^2}{T_0} \right\rangle \right. \\
+ \lambda_i \langle w_i \rangle + \int_{S_1} \gamma_{i1} (w_i^{+1} - w_i^{-1} - \frac{\partial v_i}{\partial x_1} d_1) dS_1 \\
+ \int_{S_2} \gamma_{i2} (w_i^{+2} - w_i^{-2} - \frac{\partial v_i}{\partial x_2} d_2) dS_2 \\
\left. + \int_{S_3} \gamma_{i3} (w_i^{+3} - w_i^{-3} - \frac{\partial v_i}{\partial x_3} d_3) dS_3 \right\} d\mathcal{R}
\end{aligned} \tag{10}$$

with

$$w_i^{+j} = w_i|_{y_j=d_j/2}, \quad w_i^{-j} = w_i|_{y_j=-d_j/2} \quad \text{for } j = 1, 2, 3$$

Although it is possible to carry out the variation of J_1 and find the Euler-Lagrange equations and associated boundary conditions for w_i , which results in inhomogeneous boundary conditions. It is more convenient to use change of variables to reformulate the same problem so that the boundary conditions are homogeneous. Considering the last three terms in Eq. (10), we use the following change of variables to express w_i as:

$$w_i(\mathbf{x}; \mathbf{y}) = y_j \frac{\partial v_i}{\partial x_j} + \chi_i(\mathbf{x}; \mathbf{y}) \tag{11}$$

with χ_i termed as fluctuation functions. We are free to choose the origin of the local coordinate system to be the center of UC, which implies the following constraints on χ_i :

$$\langle \chi_i \rangle = 0 \tag{12}$$

Finally, according to the variational asymptotic method (Berdichevsky, 1979), the first approximation of the variational statement in Eq. (8) can be obtained from the following functional defined over the UC:

$$\begin{aligned}
J_\Omega = \frac{1}{2} \left\langle C_{ijkl} [\bar{\epsilon}_{ij} + \chi_{(i|j)}] [\bar{\epsilon}_{kl} + \chi_{(k|l)}] \right\rangle + \frac{1}{2} \left\langle c_v \frac{\theta^2}{T_0} \right\rangle \\
+ \left\langle \beta_{ij} [\bar{\epsilon}_{ij} + \chi_{(i|j)}] \theta \right\rangle + \lambda_i \langle \chi_i \rangle \\
+ \int_{S_1} \gamma_{i1} (\chi_i^{+1} - \chi_i^{-1}) dS_1 + \int_{S_2} \gamma_{i2} (\chi_i^{+2} - \chi_i^{-2}) dS_2 \\
+ \int_{S_3} \gamma_{i3} (\chi_i^{+3} - \chi_i^{-3}) dS_3
\end{aligned} \tag{13}$$

with

$$\chi_i^{+j} = \chi_i|_{y_j=d_j/2}, \quad \chi_i^{-j} = \chi_i|_{y_j=-d_j/2} \quad \text{for } j = 1, 2, 3$$

where $\bar{\epsilon}_{ij} \equiv v_{(i,j)}$ will be shown later to be components of the global strain tensor for the structure with effective properties. The functional J_Ω in Eq. (13)

incorporates all the information for the present thermoelastic micromechanics model. This variational statement can be solved analytically for very simple cases such as binary composites (Yu and Tang, 2007), however, for general cases, we need to use computational techniques such as the finite element method (FEM) to seek numerical solutions.

3 Finite Element Implementation

It is possible to formulate the FEM solution based on Eq. (13), however, it is not the most convenient way because Lagrange multipliers will increase the number of unknowns. To this end, we can reformulate the variational statement in Eq. (13) as the minimum value of the following functional

$$\begin{aligned} \Pi_{\Omega} = \frac{1}{2\Omega} \int_{\Omega} \left\{ C_{ijkl} [\bar{\epsilon}_{ij} + \chi_{(i|j)}] [\bar{\epsilon}_{kl} + \chi_{(k|l)}] \right. \\ \left. + 2\beta_{ij} [\bar{\epsilon}_{ij} + \chi_{(i|j)}] \theta + c_v \frac{\theta^2}{T_0} \right\} d\Omega \end{aligned} \quad (14)$$

under the following nine constraints

$$\chi_i^{+j} = \chi_i^{-j} \quad \text{for } i, j = 1, 2, 3 \quad (15)$$

It is noted that Eq. (15) represents the well-known periodic boundary conditions which are assumed *a priori* in other models including MHT. while in the present model, they are derived from the variational statement in Eq. (13). The constraints in Eq. (12) do not affect the minimum value of Π_{Ω} but help uniquely determine χ_i . In practice, we can constrain the fluctuation functions at an arbitrary node to be zero and later use these constraints to recover the unique fluctuation functions. It is fine to use penalty function method to introduce the constraints in Eqs. (15). However, this method introduces additional approximation and the robustness of the solution depends on the choice of large penalty numbers. Here, we choose to make the nodes on the positive boundary surface (*i.e.*, $y_i = d_i/2$) slave to the nodes on the opposite negative boundary surface (*i.e.*, $y_i = -d_i/2$). By assembling all the independent active degrees of freedom, we can implicitly and exactly incorporate the constraints in Eqs. (15). In this way, we also reduce the total number of unknowns in the linear system which will be formulated in the following.

Introduce the following matrix notations

$$\bar{\epsilon} = [\bar{\epsilon}_{11} \quad 2\bar{\epsilon}_{12} \quad \bar{\epsilon}_{22} \quad 2\bar{\epsilon}_{13} \quad 2\bar{\epsilon}_{23} \quad \bar{\epsilon}_{33}]^T \quad (16)$$

$$\epsilon_1 = \begin{Bmatrix} \frac{\partial \chi_1}{\partial y_1} \\ \frac{\partial \chi_1}{\partial y_2} + \frac{\partial \chi_2}{\partial y_1} \\ \frac{\partial \chi_2}{\partial y_2} \\ \frac{\partial \chi_1}{\partial y_3} + \frac{\partial \chi_3}{\partial y_1} \\ \frac{\partial \chi_2}{\partial y_3} + \frac{\partial \chi_3}{\partial y_2} \\ \frac{\partial \chi_3}{\partial y_3} \end{Bmatrix} = \begin{bmatrix} \frac{\partial}{\partial y_1} & 0 & 0 \\ \frac{\partial}{\partial y_2} & \frac{\partial}{\partial y_1} & 0 \\ 0 & \frac{\partial}{\partial y_2} & 0 \\ \frac{\partial}{\partial y_3} & 0 & \frac{\partial}{\partial y_1} \\ 0 & \frac{\partial}{\partial y_3} & \frac{\partial}{\partial y_2} \\ 0 & 0 & \frac{\partial}{\partial y_3} \end{bmatrix} \begin{Bmatrix} \chi_1 \\ \chi_2 \\ \chi_3 \end{Bmatrix} \equiv \Gamma_h \chi \quad (17)$$

where Γ_h is an operator matrix and χ is a column matrix containing the three components of the fluctuation functions. If we discretize χ using the finite elements as

$$\chi(x_i; y_i) = S(y_i) \mathcal{X}(x_i) \quad (18)$$

where S representing the shape functions (in the assembled sense excluding the constrained node and slave nodes) and \mathcal{X} a column matrix of the nodal values of the fluctuation functions for all active nodes. Substituting Eqs. (16), (17), and (18) into Eq. (14), we obtain a discretized version of the functional as

$$\begin{aligned} \Pi_\Omega = & \frac{1}{2\Omega} (\mathcal{X}^T E \mathcal{X} + 2\mathcal{X}^T D_{h\epsilon} \bar{\epsilon} + \bar{\epsilon}^T D_{\epsilon\epsilon} \bar{\epsilon} \\ & + 2\mathcal{X}^T D_{h\theta} \theta + 2\bar{\epsilon}^T D_{\epsilon\theta} \theta + D_{\theta\theta} \frac{\theta^2}{T_0}) \end{aligned} \quad (19)$$

where

$$\begin{aligned} E &= \int_{\Omega} (\Gamma_h S)^T D (\Gamma_h S) d\Omega & D_{h\epsilon} &= \int_{\Omega} (\Gamma_h S)^T D d\Omega \\ D_{\epsilon\epsilon} &= \int_{\Omega} D d\Omega & D_{h\theta} &= \int_{\Omega} (\Gamma_h S)^T \beta d\Omega \\ D_{\epsilon\theta} &= \int_{\Omega} \beta d\Omega & D_{\theta\theta} &= \int_{\Omega} c_v d\Omega \end{aligned}$$

with D as the 6×6 material matrix condensed from the fourth-order elasticity tensor C_{ijkl} , and β as the 6×1 column condensed from β_{ij} . Minimizing Π_Ω in Eq. (19), we obtain the following linear system

$$E \mathcal{X} = -D_{h\epsilon} \bar{\epsilon} - D_{h\theta} \theta \quad (20)$$

It is clear from Eq. (20) that the fluctuation function \mathcal{X} is linearly proportional to $\bar{\epsilon}$ and θ , which means the solution can be written symbolically as

$$\mathcal{X} = \mathcal{X}_0 \bar{\epsilon} + \mathcal{X}_\theta \theta \quad (21)$$

Substituting Eq. (21) into Eq. (19), we can calculate the Helmholtz free energy density of the UC as

$$\Pi_\Omega = \frac{1}{2} \bar{\epsilon}^T \bar{D} \bar{\epsilon} + \bar{\epsilon}^T \bar{\beta} \theta + \frac{1}{2} \bar{c}_v \frac{\theta^2}{T_0} \quad (22)$$

with

$$\begin{aligned}\bar{D} &= \frac{1}{\Omega}(\mathcal{X}_0^T D_{h\epsilon} + D_{\epsilon\epsilon}) \\ \bar{\beta} &= \frac{1}{\Omega} \left[\frac{1}{2}(D_{h\epsilon}^T \mathcal{X}_\theta + \mathcal{X}_0^T D_{h\theta}) + D_{\epsilon\theta} \right] \\ \bar{c}_v &= \frac{1}{\Omega} [\mathcal{X}_\theta^T D_{h\theta} T_0 + D_{\theta\theta}]\end{aligned}$$

Clearly \bar{D} is the effective elastic material matrix, $\bar{\beta}$ contains the effective thermal stress coefficients, \bar{c}_v is the effective specific heat, and $\bar{\epsilon}$ contains the global strains. It is easy to infer that the effective coefficients of thermal expansion, $\bar{\alpha}$, can be obtained using the following expression.

$$\bar{\alpha} = -\bar{D}^{-1}\bar{\beta} \quad (23)$$

After obtained the effective free energy density in Eq. (22), we can use it as the constitutive model of the effective medium to carry out various macroscopic analyses under different loading and temperature conditions.

If the local fields within the UC are of interest, we can recover those fields after we have obtained the macroscopic behavior which can be described by global displacements v_i and global temperature distribution θ .

To recover the local displacement field, we need to construct two new arrays $\tilde{\mathcal{X}}_0$ and $\tilde{\mathcal{X}}_\theta$ from \mathcal{X}_0 and \mathcal{X}_θ , respectively, by assigning the values for slave nodes according to the corresponding active nodes and assign zeros to the constrained node. Obviously, $\tilde{\mathcal{X}}_0$ and $\tilde{\mathcal{X}}_\theta$ still yield the minimum value of Π_Ω in Eq. (14) under constrains in Eqs. (15). However, $\tilde{\mathcal{X}}_0$ and $\tilde{\mathcal{X}}_\theta$ may not satisfy the constraints in Eq. (12). The real solution, denoted as $\bar{\mathcal{X}}_0$ and $\bar{\mathcal{X}}_\theta$, can be found trivially by adding a constant, which is equal to the average of the fluctuation functions, to each node so that Eq. (12) is satisfied. Then the real solution of the fluctuation function is

$$\bar{\mathcal{X}} = \bar{\mathcal{X}}_0 \bar{\epsilon} + \bar{\mathcal{X}}_\theta \theta \quad (24)$$

After having determined the fluctuation functions uniquely, we can recover the local displacement using Eqs. (9), (11), and (24) as

$$u = v + \begin{bmatrix} \frac{\partial v_1}{\partial x_1} & \frac{\partial v_1}{\partial x_2} & \frac{\partial v_1}{\partial x_3} \\ \frac{\partial v_2}{\partial x_1} & \frac{\partial v_2}{\partial x_2} & \frac{\partial v_2}{\partial x_3} \\ \frac{\partial v_3}{\partial x_1} & \frac{\partial v_3}{\partial x_2} & \frac{\partial v_3}{\partial x_3} \end{bmatrix} \begin{Bmatrix} y_1 \\ y_2 \\ y_3 \end{Bmatrix} + \bar{S} \bar{\mathcal{X}} \quad (25)$$

with u as the column matrix of u_i and v as the column matrix of v_i . Here \bar{S} is different from S due to the recovery of slave nodes and the constrained node.

The local strain field can be recovered using Eqs. (6), (9), (11), (17), and (24) as

$$\epsilon = \bar{\epsilon} + \Gamma_h \bar{S} \bar{\mathcal{X}} \quad (26)$$

Finally, the local stress field can be recovered straightforwardly using the 3D constitutive relations for the constituent material as

$$\sigma = D\epsilon + \beta\theta \quad (27)$$

Both the theoretical formulation and finite element formulation can be reduced to be those of Yu and Tang (2007) if one sets $\beta_{ij} = 0$ and $c_v = 0$. It is worthy to point out that the involved recovery procedure in Yu and Tang (2007) to obtain the unique fluctuation functions in Eq. (24) is avoided by recognizing the fact the differences between $\bar{\mathcal{X}}_0$ and $\bar{\mathcal{X}}_\theta$ and $\tilde{\mathcal{X}}_0$ and $\tilde{\mathcal{X}}_\theta$ are equal to the average of the fluctuation functions calculated from $\tilde{\mathcal{X}}_0$ and $\tilde{\mathcal{X}}_\theta$.

We have implemented this formulation in the computer program VAMUCH. In the next section, we will use a few examples to demonstrate the application and accuracy of the theory and code.

4 Numerical Examples

Numerous examples including binary composites, fiber reinforced composites, and particle reinforced composites in Yu and Tang (2007) have been used to demonstrate that VAMUCH consistently achieves excellent accuracy for predicting effective elastic properties in comparison to other existing approaches. In this paper, we will use some examples to demonstrate the predictive capability of VAMUCH to recover the local stress field within the UC, and predict effective coefficients of thermal expansions and specific heats, and recover local stress field due to temperature changes.

4.1 Predict local stresses

A high-fidelity micromechanics model, such as VAMUCH, should not only provide an accurate prediction for effective properties but also recover the local displacement, stress, and strain fields within the UC, which are needed for detailed analysis.

To demonstrate the accuracy of VAMUCH in predicting the local fields, we consider the classical problem of an isotropic circular fiber embedded in an infinite isotropic matrix subjected to the uniform far-field stress σ_{22}^∞ (the so-called Eshelby problem). It is a plane strain elasticity problem and can be

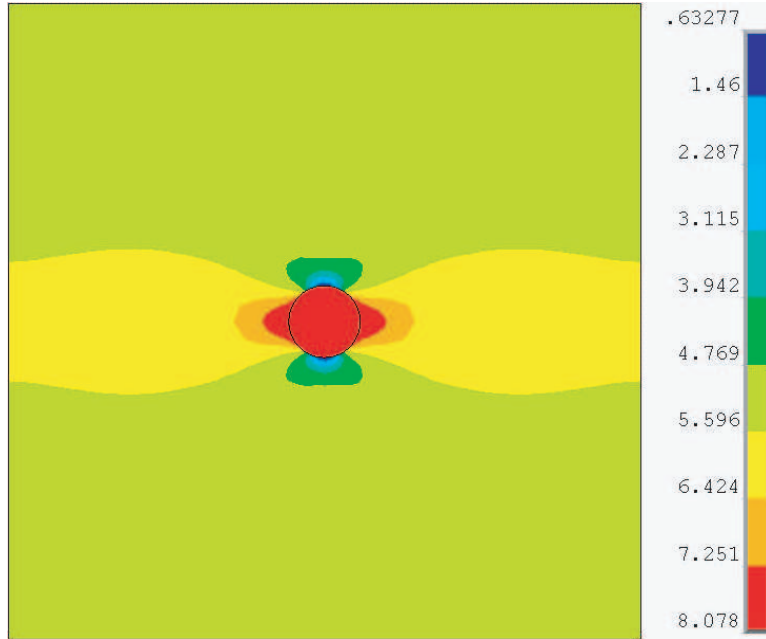


Fig. 3. Contour plot of σ_{22} (MPa) within the UC

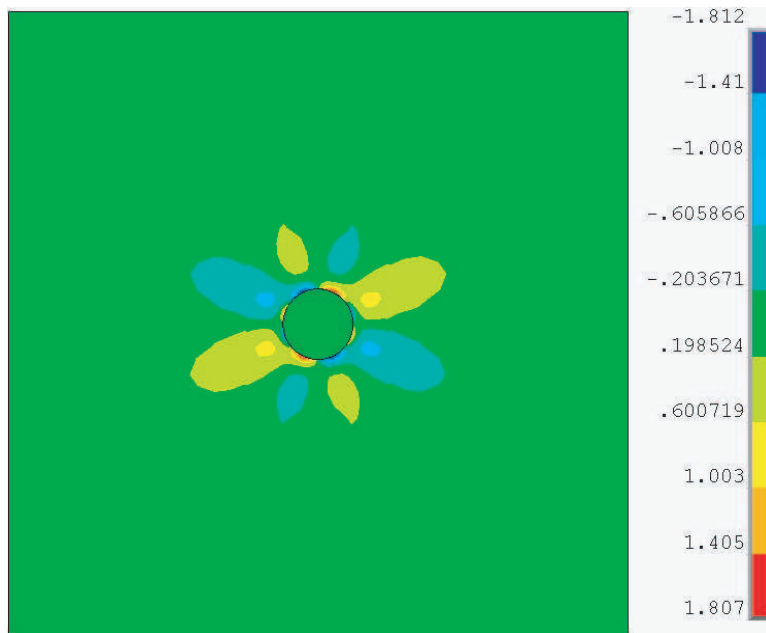


Fig. 4. Contour plot of σ_{23} (MPa) within the UC

solved exactly. The analytical formulas can be found in Aboudi et al. (2001). To mimic this dilute case, we consider a UC with sufficiently small fiber volume fraction (we choose 0.01 for this example) so that the interaction effects due to the presence of adjacent cells are negligible. Except this restriction, the exact solution provides a convenient basis to validate the accuracy of the local fields calculated using VAMUCH.

For calculation, we choose the fiber to be glass with Young's modulus $E = 69.0$ GPa and Poisson's ratio $\nu = 0.20$, the matrix to be epoxy with Young's modulus $E = 4.80$ GPa and Poisson's ratio $\nu = 0.34$. The choice of these materials produces a high elastic moduli mismatch and thus a significant disturbance in the stress field along the interface between fiber and matrix. To obtain the stress distribution within the UC, we need to run VAMUCH first to calculate the effective properties of the composite materials. It is found out that this material is transversely isotropic with $E_1 = 5.44$ GPa, $E_2 = E_3 = 4.93$ GPa, $G_{12} = G_{13} = 1.82$ GPa, $\nu_{12} = \nu_{13} = 0.338$, and $\nu_{23} = 0.357$. Then we can use these properties to solve the plane strain problem of the effective medium under the application of a far-field stress $\sigma_{22}^\infty = 5.5032$ MPa, which will generate a macroscopic strain field $\bar{\epsilon}_{22} = 0.1\%$ and $\bar{\epsilon}_{33} = -0.0514\%$ within the effective medium. Such values can be fed back to VAMUCH to recover the stress distribution within the material. Figures 3 and 4 show the contour plots for the distributions of σ_{22} and σ_{23} within the UC generated by VAMUCH. The contour plots of the exact solution in Aboudi et al. (2001) are not presented here for brevity because they are almost the same as those in Figures 3 and 4. Both stress components have sudden changes in the interface between fiber and matrix, which clearly demonstrates that VAMUCH is capable of capturing stress concentrations. Although contour plots can provide us some qualitative information, to rigorously assess the accuracy of VAMUCH, we plot σ_{22} distributions predicted by VAMUCH and the exact solution along the lines $y_2 = 0$ and $y_3 = 0$ in Figure 5 and Figure 6, respectively. It is evident that VAMUCH has an excellent agreement with the exact solution. Both the continuous condition along $y_3 = 0$ and discontinuous condition along $y_2 = 0$ are well captured by VAMUCH. The slight differences along the edges are caused by the interaction effects due to presence of adjacent cells because our far-field stress σ_{22}^∞ is not really uniform along the edges which can be observed from the contour plot in Figure 3. It has been verified that if the fiber volume fraction is as low as 0.0025, σ_{22}^∞ will be uniform along the edges and the prediction of VAMUCH is indistinguishable from the exact solutions. The discontinuity on the interface along $y_2 = 0$ in Figure 5 can be captured better if one refines the mesh in the vicinity. The results calculated using ANSYS following the approach in Sun and Vaidya (1996) are also plotted in the figures. All three sets of results are almost on the top of each other and ANSYS results are almost identical to VAMUCH results.

It is worthy to point out that local stress distribution is a critical assessment of micromechanics models and most of existing models cannot accurately predict the local stresses even though they may have excellent predictions for effective properties (Williams, 2005a). The fact that VAMUCH achieves an excellent agreement with the exact solution for local stresses clearly demonstrated the high-fidelity predictive capabilities of VAMUCH for micromechanical analysis of heterogeneous materials.

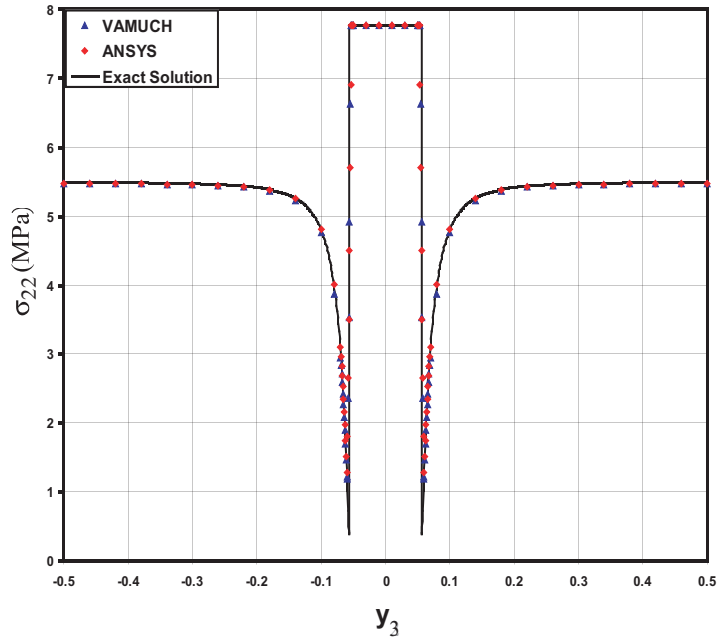


Fig. 5. Comparison of normal stress σ_{22} distribution along $y_2 = 0$

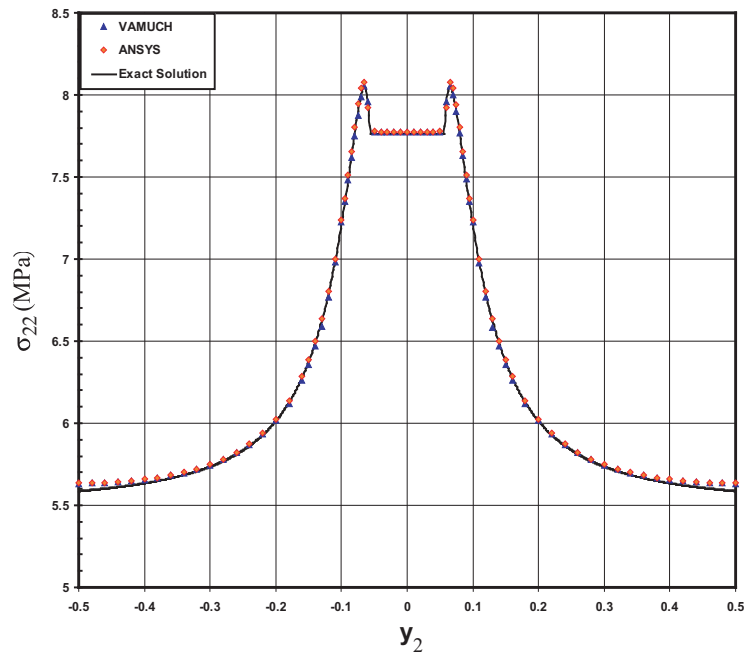


Fig. 6. Comparison of normal stress σ_{22} distribution along $y_3 = 0$

4.2 Predict effective CTEs

As reviewed by Rosen and Hashin (1970), Levin (1968) provides analytical expressions relating effective CTEs and effective elastic moduli for two phase

Table 1
Effective CTEs of boron/aluminum composites

Models	$\alpha_{11}(10^{-6}/\text{K})$	$\alpha_{22}(10^{-6}/\text{K})$
Exact Solution (Rosen and Hashin, 1970)	10.99	16.69
VAMUCH	10.99	16.69
HFGMC (Aboudi et al., 2001)	11.00	16.70
GMC (Paley and Aboudi, 1992)	10.91	16.94
Tamma and Avila (Tamma and Avila, 1999)	10.77	17.34

isotropic or transversely isotropic composites having isotropic constituents. Since there are no exact formulas existing for effective elastic moduli for general UCs and VAMUCH achieves excellent accuracy for predicting such properties (Yu and Tang, 2007), we will consider the elastic properties predicted by VAMUCH as exact and use them to calculate the effective CTEs following the analytical expressions given in Rosen and Hashin (1970). It is noted that these analytical expressions provide exact predictions for effective CTEs only if the corresponding elastic moduli are exact. Nevertheless, they are labeled as “exact solution” to indicate that the relations are given in exact closed-form expressions.

The first example is a boron/aluminum composite. Both constituents are isotropic with Young’s modulus $E = 379.3$ GPa, Poisson’s ratio $\nu = 0.1$, and CTE $\alpha = 8.1 \cdot 10^{-6}/\text{K}$ for boron fibers, and $E = 68.3$ GPa, Poisson’s ratio $\nu = 0.3$, and CTE $\alpha = 23.0 \cdot 10^{-6}/\text{K}$ for aluminum matrix. The fiber is of circular shape and arranged in a square array (see the sketch in the middle of Figure 1). The example of fiber volume fraction 0.47 is studied in several places (Aboudi et al., 2001; Tamma and Avila, 1999; Paley and Aboudi, 1992). The effective CTEs predicted by different approaches are listed in Table 1. It can be observed that VAMUCH has a perfect match with the exact solution up to the fourth significant digit. HFGMC also has an excellent agreement with the exact solution while GMC and Tamma and Avila’s results are not so accurate. To show the trend of change of effective CTEs with respect to change of the fiber volume fraction, we plot the effective CTEs for the same composite with different fiber volume fractions in Figure 7 and Figure 8. As it is expected, both axial CTEs and transverse CTEs are decreasing with increasing fiber volume fractions. Again the perfect match between exact solution and VAMUCH for various fiber volume fraction is observed.

The second example is to predict the effective CTE for a glass/epoxy particle reinforced composite. The UC of this composite is composed of glass spheres embedded in a triply periodic cubic array. Both constituents are isotropic with Young’s modulus $E = 72.38$ GPa, Poisson’s ratio $\nu = 0.2$, and CTE $\alpha = 5.0 \cdot 10^{-6}/\text{K}$ for glass, and Young’s modulus $E = 2.75$ GPa, Poisson’s

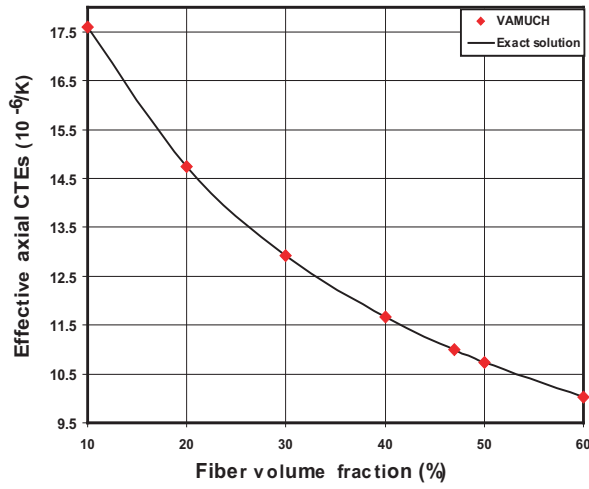


Fig. 7. Change of effective α_{11} of the boron/aluminum composite with respect to fiber volume fractions

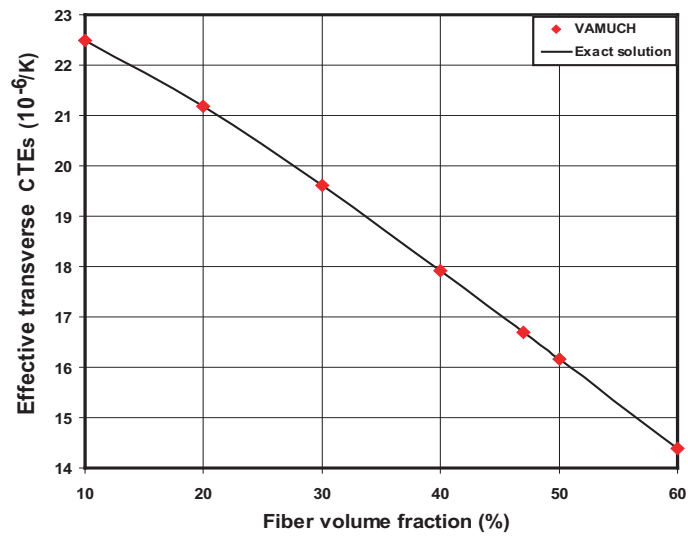


Fig. 8. Change of effective α_{22} of the boron/aluminum composite with respect to fiber volume fractions

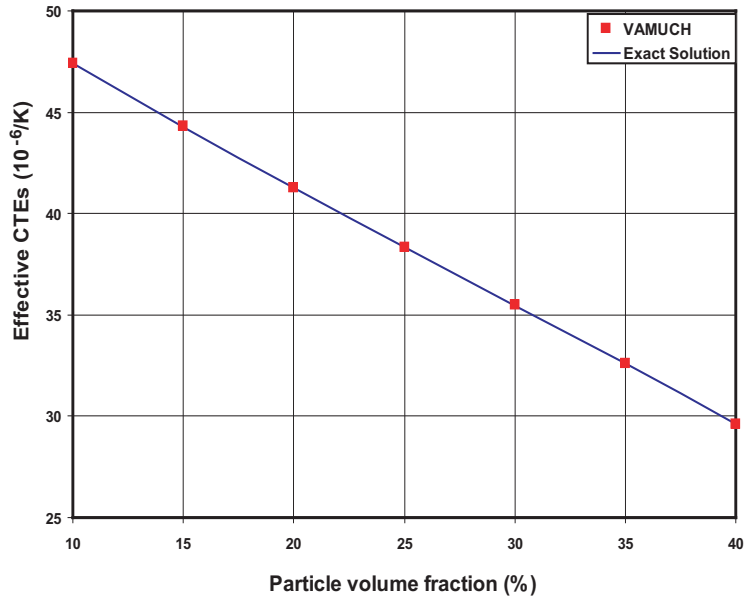


Fig. 9. Change of effective CTEs of the glass/epoxy composite with respect to spherical inclusion volume fractions

ratio $\nu = 0.35$, and CTE $\alpha = 54.0 \cdot 10^{-6}/\text{K}$ for epoxy. It is noticed that the properties are directly taken from Aboudi (1984) and different from those in Section 4.1. We plot the change of effective CTE with respect to the particle volume fractions in Figure 9. It is found out that VAMUCH results are right on the top of the exact solution, which demonstrates VAMUCH provides accurate predictions for CTEs for particle reinforced composites.

To demonstrate the application and accuracy of the present model for more realistic heterogeneous materials, we choose a more complex microstructure as shown in Figure 10. Within one UC, the reinforcements are a square fiber and a thin-wall frame around the square fiber. Both matrix and reinforcements are isotropic with Young's modulus $E = 100000 \text{ MPa}$, Poisson's ratio $\nu = 0.32$, and CTE $\alpha = 10.0 \cdot 10^{-12}/\text{K}$ for reinforcements, while the Young's modulus of matrix takes different values from 10 MPa, 100 MPa, 1000 MPa, 10000MPa, and 50000MPa and its Poisson's ratio and CTE are fixed at 0.49 and $\alpha = 4.0 \cdot 10^{-6}/\text{K}$, respectively. The contrast ratio of CTEs of two constituents is as high as 4×10^5 . There are no analytical solution for composites with this kind of microstructure. To validate the present model, we use ANSYS, a commercial finite element code, to carry out a thermoelastic micromechanics analysis following the approach of Sun and Vaidya (1996). Table 2 shows the effective CTEs of composites of different matrix predicted by VAMUCH and ANSYS. It can be seen that the predictions of VAMUCH are almost the same as those obtained from ANSYS at different contrast ratios of Young's modulus of the constituents.

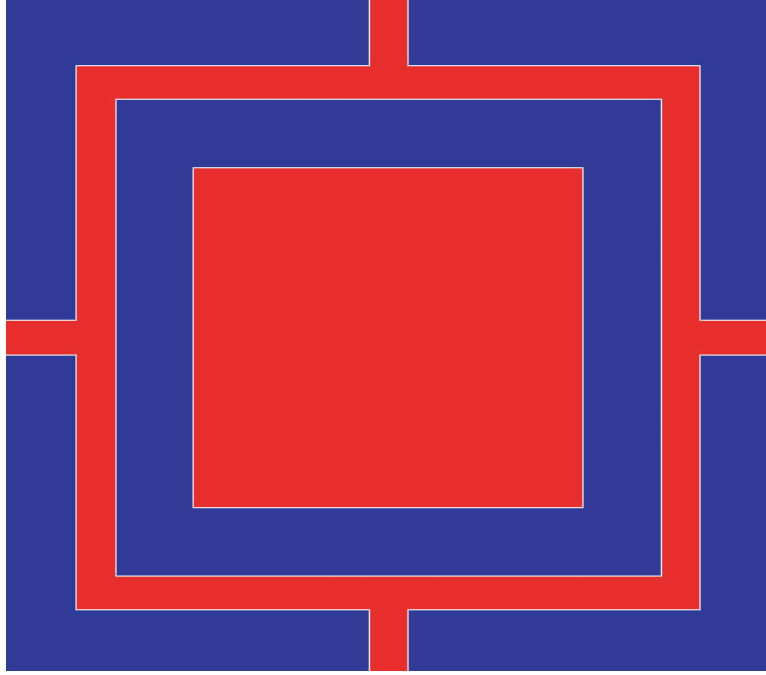


Fig. 10. Sketch of a complex microstructure

Table 2
Effective CTEs of frame shape composites

Matrix Young's Modulus	α_{11} ($10^{-9}/\text{K}$)		α_{22} ($10^{-6}/\text{K}$)	
	VAMUCH	ANSYS	VAMUCH	ANSYS
$E_m = 10$ MPa	3.92	3.90	2.22	2.23
$E_m = 100$ MPa	14.6	14.6	3.12	3.28
$E_m = 1000$ MPa	97.1	97.0	3.12	3.28
$E_m = 10000$ MPa	637	637	3.23	3.23
$E_m = 50000$ MPa	1886	1886	2.886	2.886

4.3 Predict effective specific heat

Rosen and Hashin (1970) derived closed-form expressions for macroscopically isotropic composites having two isotropic phases and bounds for macroscopically anisotropic composites relating effective specific heat and elastic moduli. Again, although those relations are in closed-form, they can predict the exact effective specific heat only if the elastic moduli predictions are exact. Here we use the elastic properties predicted by VAMUCH in these relations and label them as “exact solution” only to reflect the fact that the effective specific heats are obtained from closed-form expressions.

First, we use a steel/aluminum particle reinforced composite which can be

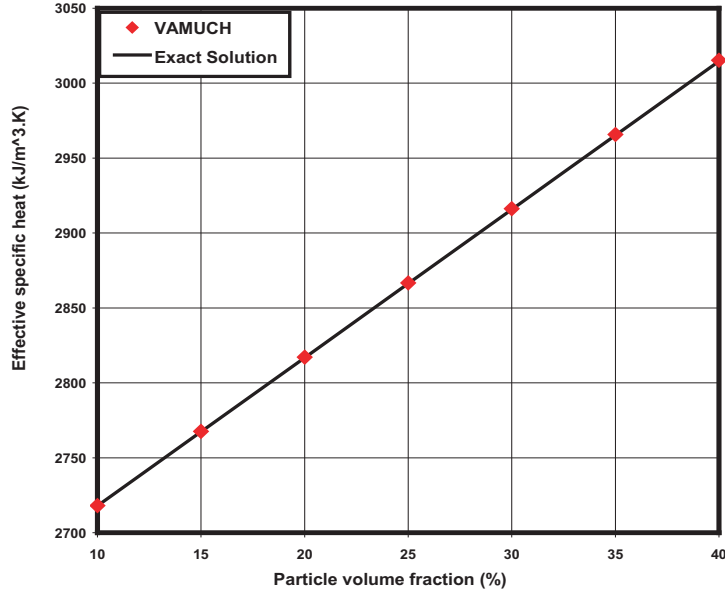


Fig. 11. Effective specific heat c_v of steel/aluminum composite varies with particle volume fraction

considered as macroscopically isotropic. Both constituents are isotropic with $E = 200$ GPa, $\nu = 0.3$, $\alpha = 12 \cdot 10^{-6}/\text{K}$, and $c_v = 3609.6$ kJ/(m³·K) for steel particles, and $E = 68.3$ GPa, $\nu = 0.3$, $\alpha = 23.0 \cdot 10^{-6}/\text{K}$, and $c_v = 2619.1$ kJ/(m³·K) for aluminum matrix. To examine the agreement of VAMUCH with respect to the exact relations (Rosen and Hashin, 1970), we plot the effective specific heat c_v with different steel volume fraction as shown in Figure 11. It can be seen that the VAMUCH results have an excellent match with the exact relations (Rosen and Hashin, 1970).

To show that VAMUCH can also predict the effective specific heat for macroscopically anisotropic composites, we chose the silicon carbide fiber reinforced copper matrix (SiC/Cu) composite as an example. Both constituents are also isotropic with $E = 410$ GPa, $\nu = 0.14$, $\alpha = 4.0 \cdot 10^{-6}/\text{K}$, and $c_v = 2327.73$ kJ/(m³·K) for silicon carbide fibers, and $E = 117$ GPa, $\nu = 0.34$, $\alpha = 22.0 \cdot 10^{-6}/\text{K}$, and $c_v = 3485.09$ kJ/(m³·K) for copper matrix. Only bounds are available for this type of composites. We plot the VAMUCH results along with the upper and lower bounds provided in Rosen and Hashin (1970) in Figure 12. It can be observed that for this composite the lower and upper bounds are very close to each other and VAMUCH results are nicely located between the bounds.

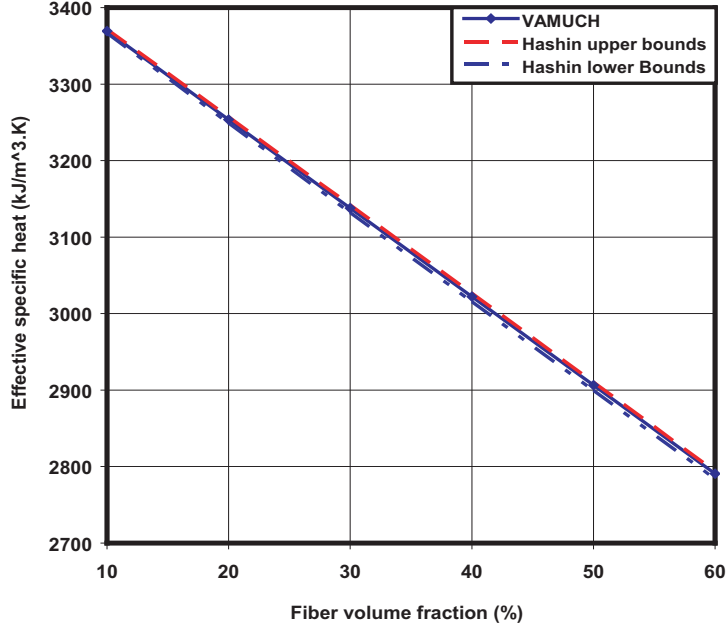


Fig. 12. Effective specific heat c_v of SiC/Cu composite varies with particle volume fraction

4.4 Predict local thermal stresses

Finally, we can use VAMUCH to recover the stress distribution within the UC due to macroscopic temperature change. Consider the boron/aluminum composite with fiber volume fraction as 0.2. We use the effective thermoelastic properties to carry out a macroscopic thermoelastic analysis of the homogenized material. Suppose we know for a certain UC, it is stress free, yet the temperature is increased by 100 K. Due to the mismatch of CTEs of the constituents, thermal stresses will be generated within the UC. The distributions of σ_{22} and σ_{23} are plotted in Figures 13 and 14, respectively. All the sudden changes of stress distributions along the fiber-matrix interface have been well captured by VAMUCH. We have also carried out a thermoelastic micromechanics analysis following the approach of Sun and Vaidya (1996) to analyze 3D RVEs using ANSYS. The local thermal stress distributions along $y_3 = 0$ and $y_2 = 0$ are plotted in Figures 15 and 16, respectively. Excellent match between these two approaches can be clearly observed from the plots. However, only 2D UCs are needed for VAMUCH to obtain these results. Such a capability of VAMUCH is useful for predicting residual stresses caused by temperature changes during manufacturing or operating processes.

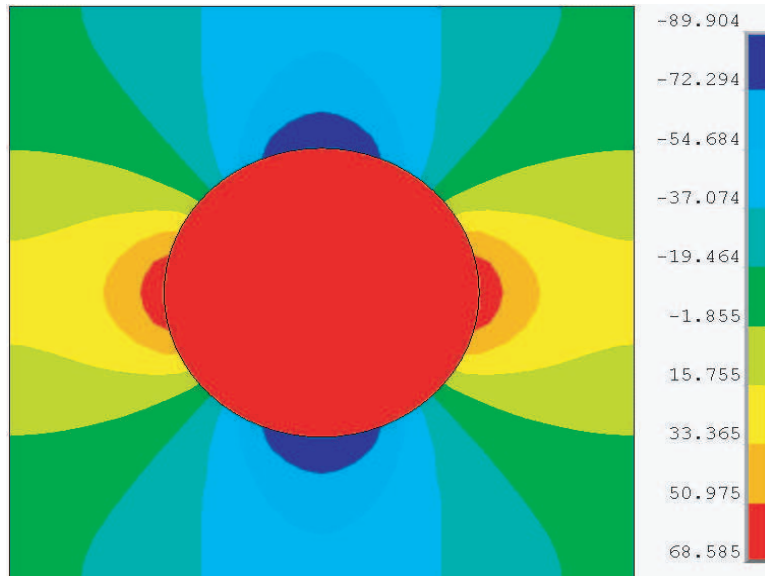


Fig. 13. Contour plot of σ_{22} (MPa) within the UC of a boron/aluminum composite due to temperature increase of 100 K

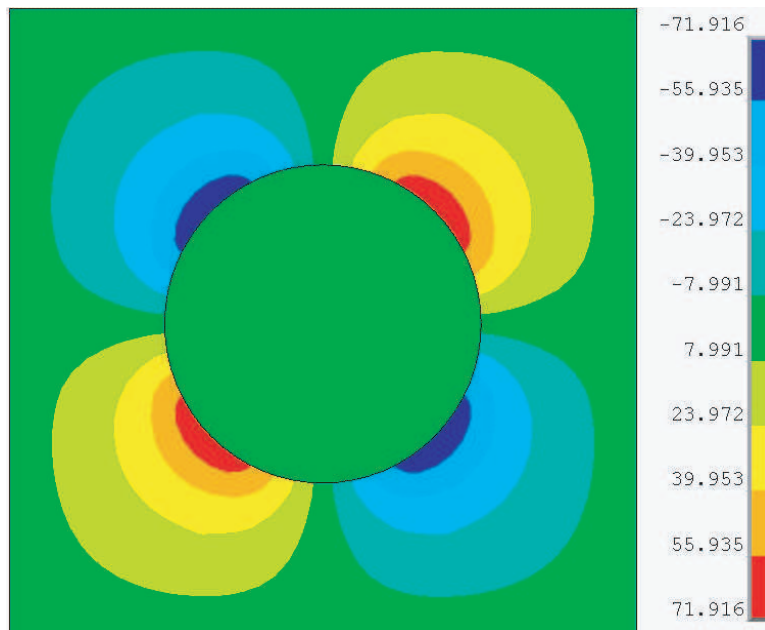


Fig. 14. Contour plot of σ_{23} (MPa) within the UC of a boron/aluminum composite due to temperature increase of 100 K

5 Conclusions

A variational asymptotic model has been developed for thermoelastic micromechanical analysis of heterogeneous materials. This model can homogenize the composite materials to find effective thermoelastic properties including elastic properties, coefficients of thermal expansion, and specific heat

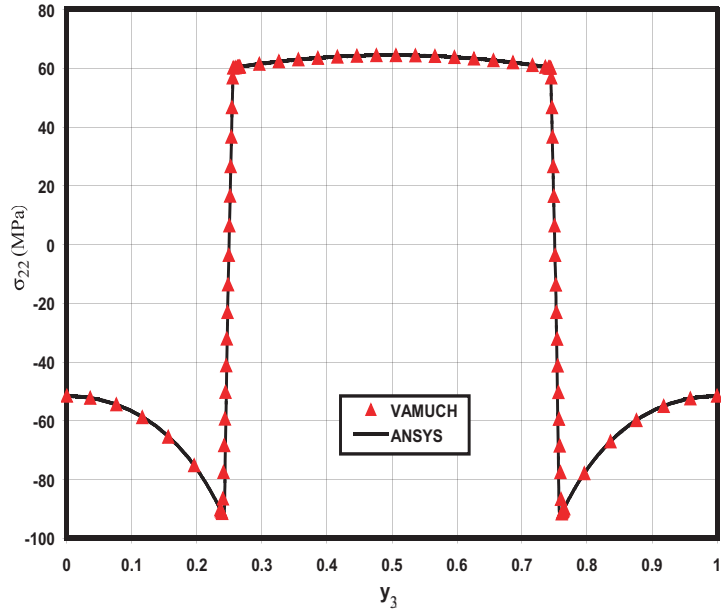


Fig. 15. Comparison of thermal stress σ_{22} distribution along $y_2 = 0$

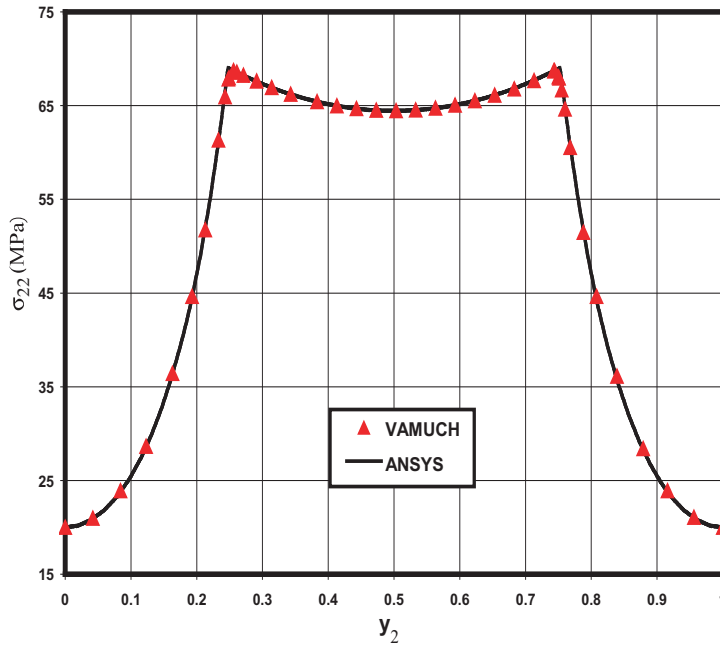


Fig. 16. Comparison of thermal stress σ_{22} distribution along $y_3 = 0$

and recover the local fields within the microstructure in terms of the global responses of the material. This model provides a uniform treatment for microstructures which can be described using 1D, 2D, or 3D UCs, such as binary composites, fiber-reinforced composites, and particle-reinforced composites. In comparison to existing micromechanics models, this model has the following

unique features:

- (1) It adopts the variational asymptotic method as its mathematical foundation. It has the same rigor as MHT without even assuming periodic fluctuation functions and boundary conditions.
- (2) It has an inherent variational nature and its numerical implementation is shown to be straightforward.
- (3) It handles 1D/2D/3D unit cells uniformly. The dimensionality of the problem is determined by that of the periodicity of the unit cell.

The present theory is implemented in the computer code, VAMUCH, which has the following advantages in comparison to FEM using conventional stress analysis of RVE (Sun and Vaidya, 1996):

- (1) VAMUCH can obtain different material properties in different directions simultaneously, which is more efficient than those approaches requiring multiple runs under different loading conditions.
- (2) VAMUCH calculates effective properties and local fields directly with the same accuracy as the fluctuation functions. No postprocessing calculations which introduces more approximations, such as averaging stresses and averaging strains, are needed.
- (3) VAMUCH can model composite materials with full anisotropy, while FEM can only handle at most macroscopically orthotropic material, which is an unnecessary restriction.

The application and accuracy of VAMUCH for predicting effective thermoelastic properties and local fields have been demonstrated through various examples.

6 Acknowledgements

This study is supported by the National Science Foundation under Grant DMI-0522908. The views and findings contained herein are those of the authors and should not be interpreted as necessarily representing the official policies or endorsement, either expressed or implied, of the National Science Foundation.

References

- Aboudi, J., 1982. A continuum theory for fiber-reinforced elastic-visoplastic composites. *International Journal of Engineering Science* 20 (5), 605 – 621.
- Aboudi, J., 1984. Effective thermal constants of short fiber composites. *Fibre Science and Technology* 20, 211 – 225.

- Aboudi, J., 1989. Micromechanical analysis of composites by the method of cells. *Applied Mechanics Reviews* 42 (7), 193 – 221.
- Aboudi, J., Pindera, M. J., Arnold, S. M., 2001. Linear thermoelastic higher-order theory for periodic multiphase materials. *Journal of Applied Mechanics* 68, 697–707.
- Accorsi, M. L., Nemat-Nasser, S., 1986. Bounds on the overall elastic and instantaneous elastoplastic moduli of periodic composites. *Mechanics of Materials* 5 (3), 209 – 220.
- Banerjee, B., Adams, D. O., 2004. On predicting the effective elastic properties of polymer bonded explosives using the recursive cell method. *International Journal of Solids and Structures* 41 (2), 481 – 509.
- Bensoussan, A., Lions, J., Papanicolaou, G., 1978. *Asymptotic Analysis for Periodic Structures*. North-Holland, Amsterdam.
- Berdichevsky, V. L., 1979. Variational-asymptotic method of constructing a theory of shells. *PMM* 43 (4), 664 – 687.
- Dvorak, G. J., Bahei-El-Din, Y. A., 1979. Elastic-plastic behavior of fibrous composites. *Journal of Mechanics and Physics of Solids* 27, 51–72.
- Hashin, Z., 1983. Analysis of composite materials—a survey. *Applied Mechanics Review* 50, 481–505.
- Hashin, Z., Shtrikman, S., 1962. A variational approach to the theory of the elastic behaviour of polycrystals. *Journal of Mechanics and Physics of Solids* 10, 343–352.
- Hill, R., 1952. The elastic behavior of crystalline aggregate. *Proc. Phys. Soc. London* A65, 349–354.
- Hill, R., 1965. Theory of mechanical properties of fibre-strengthened materials—iii. self-consistent model. *Journal of Mechanics and Physics of Solids* 13, 189–198.
- Kunin, I., 1982. *Theory of Elastic Media with Microstructure*. Vol. 1 and 2. Springer Verlag.
- Levin, V. M., 1968. Thermal expansion coefficients of heterogeneous materials. *Mekhanika Tverdogo Tela* 2 (1), 88 – 94.
- Milton, G. W., 1981. Bounds on the electromagnetic, elastic and other properties of two component composites. *Physics Review Letters* 46 (8), 542 – 545.
- Murakami, H., Toledano, A., 1990. A higher-order mixture homogenization of bi-laminated composites. *Journal of Applied Mechanics* 57, 388–396.
- Paley, M., Aboudi, J., 1992. Micromechanical analysis of composites by the generalized cells model. *Mechanics of Materials* 14, 127–139.
- Rosen, B. W., Hashin, Z., 1970. Effective thermal expansion coefficients and specific heats of composite materials. *International Journal of Engineering Science* 8, 157 – 173.
- Schapery, R. A., 1968. Thermal expansion coefficients of composite materials based on energy principles. *Journal of Composite Materials* 2, 380 – 404.
- Sun, C. T., Vaidya, R. S., 1996. Prediction of composite properties from a representative volume element. *Composites Science and Technology* 56, 171

- Tamma, K. K., Avila, A. F., 1999. An integrated micro/macro modeling and computational methodology for high temperature composites. In: Hetnarski, R. B. (Ed.), *Thermal Stresses 5*. Lastran Corporation, Rochester, NY, pp. 143–256.
- Williams, T. O., 2005a. A three-dimensional, higher-order, elasticity-based micromechanics model. *International Journal of Solids and Structures* 42, 971–1007.
- Williams, T. O., 2005b. A two-dimensional, higher-order, elasticity-based micromechanics model. *International Journal of Solids and Structures* 42, 1009–1038.
- Yu, W., Tang, T., 2007. Variational asymptotic method for unit cell homogenization of periodically heterogeneous materials. *International Journal of Solids and Structures* 44, 3738–3755.